

Decay of 3.912-h  $^{133}\text{La}$  to  $^{133}\text{Ba}$  and level structure of the  $N = 77$  nuclei\*

E. A. Henry and R. A. Meyer

Lawrence Livermore Laboratory, University of California, Livermore, California 94550

(Received 20 October 1975)

The levels of  $^{133}\text{Ba}$  populated from  $\beta$  decay of mass-separated  $^{133}\text{La}$  were studied by  $\gamma$ -ray spectroscopy and a  $\gamma$ - $\gamma$ -coincidence experiment. Discrepancies in the literature on  $^{133}\text{Ba}$  excited levels were resolved and the  $^{133}\text{Ba}$  level scheme was extended. The observed positive parity levels are qualitatively accounted for in a weak-coupling model.

RADIOACTIVITY  $^{133}\text{La}$  [from decay of  $^{133}\text{Ce}$  produced by  $\text{Ba}(\alpha, Xn)$ ] measured  $E\gamma$ ,  $I\gamma$ ,  $\gamma$ - $\gamma$  coin; deduced  $\log ft$ .  $^{133}\text{Ba}$  deduced levels,  $J$ ,  $\pi$ , ICC. Mass separation, chem.

## I. INTRODUCTION

The  $N = 77$  isotones have been studied experimentally from near the proton shell closure at  $^{129}\text{Te}$  to the levels of  $^{139}\text{Sm}$ , 12 protons beyond shell closure. Thus the influence of the core on the odd neutron can be studied over a wide range of  $Z$ . The  $^{133}\text{Ba}$  nucleus is central to these systematics because it is located midway between the  $Z = 50$  shell closure and  $^{137}\text{Nd}$ , which possesses a rotation aligned structure.<sup>1</sup> Unfortunately, little precise information on this central  $^{133}\text{Ba}$  nucleus exists. Its levels and their decay properties are poorly known, as pointed out in the recent compilation of nuclear data for the  $A = 133$  mass chain,<sup>2</sup> which reveals two studies of  $^{133}\text{La}$   $\beta$  decay and one study of the  $(d, p)$  reaction leading to levels in  $^{133}\text{Ba}$ . Our study was stimulated by the success of the particle-plus-asymmetric-rotor model in treating nearby nuclei and by the discrepancies discussed in the *Nuclear Data Sheets* for  $A = 133$ . The systematics of the level structure in these nuclei must be clarified to define the region where deformation has an important role in determining nuclear properties.

In 1966 Harmatz and Handley<sup>3</sup> studied the conversion electrons following  $^{133}\text{La}$  decay and deduced a level scheme for  $^{133}\text{Ba}$  based on energy sums. In 1973 Reuland and Pagliughi<sup>4</sup> reported on the  $\gamma$  rays resulting from the decay of  $^{133}\text{La}$ . Using NaI detectors, they performed a limited  $\gamma$ - $\gamma$  coincidence experiment to aid in developing a level scheme for  $^{133}\text{Ba}$ . The level scheme developed in these two studies agreed on 12 of 23 proposed excited levels in  $^{133}\text{Ba}$ .

In a  $(d, p)$  reaction study, von Ehrenstein *et al.*<sup>5</sup> observed five of the low-lying levels found by  $\beta$  decay, reported two low-lying levels not seen in  $\beta$  decay, and established approximately 10 addi-

tional excited levels above 1200 keV. However, the  $l$ -transfer values for some levels are not consistent with the spin and parity assignments deduced from  $\beta$  decay. For example, the  $l$ -transfer value of 1 reported for the population of a level at 858 keV was not consistent with the proposal of Reuland and Pagliughi that  $J^\pi = \frac{3}{2}^+$  for that level.

Our work was undertaken to resolve such discrepancies and to further explore the level structure of  $^{133}\text{Ba}$ .

## II. EXPERIMENTAL METHODS

Our experiment was done in conjunction with experiments designed to study the  $\beta$  decay of  $^{133}\text{Ce}$ . Because  $^{133}\text{La}$  is the daughter product of  $^{133}\text{Ce}$  decay,  $^{133}\text{Ce}$  was produced in the 224-cm cyclotron at the Lawrence Berkeley Laboratory with the  $(\alpha, 3n)$  reaction on  $\text{BaCO}_3$  targets enriched in  $^{132}\text{Ba}$ . The targets were transported to Lawrence Livermore Laboratory where the cerium was chemically separated from the barium target material.<sup>6</sup> The cerium was then mass separated onto aluminum foil. The  $^{133}\text{Ce}$  sources were counted with large-volume Ge(Li) detectors and a low-energy photon spectrometer (LEPS) for which efficiency and linearity were routinely calibrated. The  $^{133}\text{La}$  daughter grew into near transient equilibrium with the  $^{133}\text{Ce}$  in these sources. Energy calibration of the intense  $^{133}\text{La}$   $\gamma$  rays was made by counting one source simultaneously with  $^{182}\text{Ta}$ ,  $^{133}\text{Ba}$ ,  $^{56}\text{Co}$ ,  $^{110}\text{Ag}^m$ , and  $^{113}\text{Sn}$ .

To positively identify the  $\gamma$  rays resulting from  $^{133}\text{La}$  decay, a lanthanum-cerium separation was performed.<sup>6</sup> The lanthanum fraction was counted with large-volume Ge(Li) detectors and the LEPS detector. The low-intensity  $^{133}\text{La}$   $\gamma$  rays were calibrated against the high-intensity  $\gamma$  rays in these spectra. The lanthanum-free  $^{133}\text{Ce}$  source

was counted again to further confirm the assignment of the  $\gamma$  rays. The  $\gamma$  ray singles spectra were analyzed using the computer code GAMANAL.<sup>7</sup>

A portion of the  $^{133}\text{La}$  source was used to make a precision measurement of the half-life of  $^{133}\text{La}$ . This measurement used an automated counting device that followed the decay of  $^{133}\text{La}$  for more than 10 half-lives. The instrument and analysis techniques are described elsewhere.<sup>8</sup>

$\gamma$ - $\gamma$ -coincidence counting was done with the megachannel coincidence system in conjunction with a PDP-9 computer.<sup>9</sup> Coincidences from a mixed source of  $^{133}\text{Ce}$  and  $^{133}\text{La}$  were detected with two 30-cm<sup>3</sup> Ge(Li) detectors in a 90° configuration. Lead absorbers between the detectors reduced the crystal-to-crystal scattering. A standard slow-fast coincidence system was used with a timing window of approximately 100 ns. Coincidences were stored event by event on a disk for later on-line analysis.<sup>9</sup> Chance coincidences were automatically corrected for by setting a second timing window away from the timing peak. The total coincidence rate of approximately 150 coincidences per second had a true-to-chance ratio of approximately 12 to 1.

During analysis of the coincidence data using the PDP-9, 3- to 6-keV-wide  $\gamma$ -ray gates were set on the spectrum from one of the detectors. A nearby Compton-background gate of equal width was subtracted from the  $\gamma$ -ray gate. The resulting spectrum was then analyzed with GAMANAL to obtain

coincident  $\gamma$  rays and scanned visually for weak coincidences of particular interest.

### III. DATA AND RESULTS

Portions of the  $^{133}\text{La}$   $\gamma$ -ray singles spectrum are quite complex. Figure 1 shows a region of the cerium-free lanthanum spectrum near 600 keV. Several of the closely spaced doublets and interspersed weak photopeaks are not reported in previous studies. For example, Reuland and Pagliughi did not resolve the 565- and 567-keV doublet or the 630- and 632-keV doublet.<sup>4</sup>

Approximately 129  $\gamma$  rays were assigned to  $^{133}\text{La}$  decay, including 7 tentative assignments and the 276-keV isomeric transition in  $^{133}\text{Ba}$ . The 12.33-keV transition from the  $^{133}\text{Ba}$  first excited state was observed in LEPS spectra; however, the calibration of the detector at this low energy is not accurate enough for reliable intensity data. The  $\gamma$ -ray energies, relative intensities, and placements are summarized in Table I.

Conversion coefficients were determined for many of the more intense transitions with the conversion electron intensities of Handley and Haratz. Normalization assumes  $\alpha_k(278\gamma) = 0.0487$ : the conversion coefficient for an equal mixture of  $M1$  and  $E2$  multipolarity. It is at most 5% uncertain if the transition is pure  $M1$  or pure  $E2$ . This contribution to the total uncertainty is substantially smaller than that from the  $\pm 15\%$  uncertainty in the intensity of the most intense conversion electron peaks. The calculated conversion coefficients and multiplicities deduced by comparison with theoretical values from Hager and Seltzer<sup>10</sup> are given in Table II.

The coincidence results are summarized in Table III.

The half-life of  $^{133}\text{La}$  was determined from samples first mass separated and then chemically separated from  $^{133}\text{Ce}$ . The resulting value for the  $^{133}\text{La}$  half-life is  $3.912 \pm 0.008$  h.<sup>8,11</sup>

We determined the  $^{133}\text{Ba}$  level scheme shown in Fig. 2.  $\gamma$ -ray energy sums and coincidence data were used to place 96  $\gamma$  rays into the  $^{133}\text{Ba}$  level scheme with 27 excited levels. Nine additional  $\gamma$  rays are tentatively placed in this level scheme, including  $\gamma$  rays with more than one possible placement. Of the excited levels, 16 have at least one coincidence to support their existence. All remaining levels (except the isomeric level and the 1284.0-keV level that are based on a single transition) are based on two or more energy sums. No  $\gamma$  ray is seen in the coincidence spectrum when a gate is placed on the 1284.0-keV  $\gamma$  ray. Thus, this  $\gamma$  ray populates either the ground state or the 12.33-keV level. Because a level was observed at

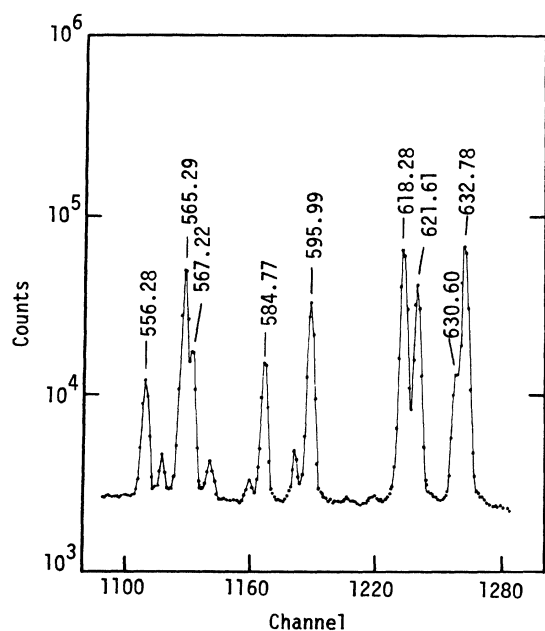


FIG. 1. A portion of the cerium-free lanthanum spectrum near 600 keV taken with large-volume Ge(Li) detector.

TABLE I. Energies, relative intensities, and placements for  $\gamma$  rays resulting from  $^{133}\text{La}$  decay.

$E\gamma(\Delta E\gamma)$	$I\gamma(\text{rel.})(\Delta I\gamma)$	Placement From-To	$E\gamma(\Delta E\gamma)$	$I\gamma(\text{rel.})(\Delta I\gamma)$	Placement From-To
12.33 <sup>a</sup>		12-0	721.9(3)	1.8(4)	1352-630
113.6(3)	2.1(3)		733.5	1.1(5)	1620-887
136.7(2)	0.8(3)		751.8(3)	22.7(8)	1329-577
158.4(3)	0.7(3)	1021-862?	775.3(3)	1.7(4)	1352-577
210.72(12)	2.5(5)	887-676	802.3(4)	1.2(6)	1689-887
227.85(10)	3.0(5)	858-630	810.3(2)	22.3(15)	1112-302
256.57(6)	9.1(6)	887-630	821.1(3)	6.9(6)	1112-291
278.83(3)	1000(3)	291-12	846.16(13)	250(7)	858-12
281.8(2)	5(2)		848.4(3)?	3.4(7)	1707-858?
286.34(5)	12.2(11)	577-291	850.5(2)	14.2(8)	862-12
290.06(5)	565(5)	302-12	858.50(13)	202(6)	858-0
291.17(5)	174(3)	291-0	874.8(2)	29.1(9)	887-12
293.17(11)	10(2)	923-630?	887.1(2)	14.2(7)	887-0
302.38(4)	654(5)	302-0	891.9(3)	1.2(4)	
309.50(10)	4.1(11)	887-577	909.5(3)	4.1(9)	1211-302
324.63(12)	3.1(8)	1211-887	911.6(2)	70(2)	923-12
328.17(7)	10.6(8)	630-302	920.7(2)	8.9(5)	1211-291
339.41(8)	21(3)	630-291	923.9(2)	9.0(5)	923-0
345.1(4)?	0.6(5)	1021-676?	933.0(2)	5.8(7)	1563-630
347.1(3)	1.3(6)	887-539	981.0(3)	2.1(4)	
353.26(9)	7.6(7)	1211-858	992.8(3)	2.7(6)	
374.13(15)	2.4(7)	676-302	1009.30(10)	37.7(11)	1021-12
385.25(9)	27.1(8)	676-291	1021.6(2)	3.0(5)	1021-0
428.7(2)	1.7(6)	1352-923	1038.1(2)	3.9(5)	1329-291
432.3(3)?	0.9(5)		1043.0(2)	4.2(5)	1620-577
435.77(10)	10.4(11)	1112-676	1061.48(10)	41.8(13)	1352-291
441.9(4)?	0.7(5)	1329-887?	1080.9(4)	0.7(3)	1620-539
445.5(3)	1.7(10)	1329-883	1099.93(13)	100(3)	1112-12
465.53(11)	4.2(6)	1352-887	1111.9(4)	0.9(4)	{ 1689-577? 1112-0?
469.3(3)	8.7(7)	1352-883	1175.7(2)	2.5(4)	
481.75(8)	17.5(10)	1021-539	1182.2(3)	1.0(4)	
494.5(3)	1.2(6)	1352-858?	1192.3(3)	0.6(3)	
511 <sup>b</sup>	4576(106)		1199.5(3)	12.3(6)	1211-12
519.1(4)	9(3)		1211.8(2)	22.5(7)	1211-0
527.51(8)	34.7(9)	539-12	1219.5(3)	0.7(3)	
534.83(12)	22.0(7)	1112-577	1229.9(3)	1.7(4)	1532-302
541.3(3)	0.9(5)		1241.0(3)	1.1(4)	1532-291
556.28(8)	51.5(9)	858-302	1261.0(3)	12.5(7)	1563-302
560.25(15)	9.0(8)	862-302	1284.0(3)	33.7(12)	1284-0
565.29(7)	269(4)	577-12	1317.2(3)	13.1(8)	1329-12
567.22(7)	86(2)	858-291	1329.4(3)	3.5(4)	{ 1329-0 1620-291?
571.9(3) <sup>c</sup>	9.9(10)	862-291	1340.2(3)	1.8(3)	1352-12
581.3(2)	4.8(6)	1211-630	1387.3(3)	2.3(4)	1689-302
584.77(8)	82(2)	887-302	1398.5(3)	2.0(4)	1689-291
592.18(15)	12.5(8)	883-291	1404.7(4)	1.1(3)	1707-302
595.99(14)	189(4)	887-291	1415.9(3)	1.9(4)	1707-291
604.9(3)	1.3(6)		1467.8(4)	0.7(4)	1769-302
618.29(12)	422(8)	630-12	1478.5(4)	0.7(4)	1769-291
621.61(9)	258(6)	923-302	1516.1(5)	0.3(2)	1528-12
630.60(8)	66(2)	630-0	1528.5(4)	2.0(4)	1528-0
632.78(40)	462(7)	923-291	1540.0(4)	0.9(3)	
652.99(15)	3.9(7)	1329-676	1551.1(4)	5.6(4)	1563-12
664.21(13)	37.7(10)	676-12	1563.4(3)	4.6(3)	1563-0
671.80(12)	16.3(8)	1211-539	1581.7(4)	0.4(2)	
676.50(14)	14.1(7)	676-0	1595.6(5)?	0.3(2)	
682.0(5)	0.9(5)		1608.35(13)	23.0(9)	1620-12
684.3(5)	0.8(5)		1620.9(4)	0.5(2)	1620-0
689.5(3)	1.0(5)				
719.4(3)	1.9(5)	1021-302			

TABLE I (Continued)

$E\gamma(\Delta E\gamma)$	$I\gamma(\text{rel.})(\Delta I\gamma)$	Placement From-To	$E\gamma(\Delta E\gamma)$	$I\gamma(\text{rel.})(\Delta I\gamma)$	Placement From-To
1659.6(5)	0.5(2)		1782.9(5)	0.5(3)	
1677.3(3)	1.9(3)	1689-12	1805.6(5)	0.2(1)	
1694.6(4)	2.5(3)	1707-12	1818.1(4)	0.5(1)	1830-12
1706.7(4)	0.5(2)	1707-0	1830.2(3)	0.6(2)	1830-0
1720.2(2)	0.3(2)		1851.7(6)?	0.2(1)	
1757.2(4)	0.8(2)	1769-12	1886.7(4)?	0.3(1)	
1769.4(3)	3.6(4)	1769-0			

<sup>a</sup> Energy deduced from cascade and crossover  $\gamma$ -ray energy differences; energy of 12.2 keV obtained using LEPS.

<sup>b</sup> Annihilation radiation.

<sup>c</sup> Peak width indicates a possible doublet.

1286 keV in the ( $d, p$ ) study of von Ehenstein *et al.*, this  $\gamma$  ray is placed feeding the ground state.

The 276-keV isomeric transition depopulates the 38.9-h isomeric level in  $^{133}\text{Ba}$  and is observed in  $^{133}\text{La}$  spectra taken at late times (Fig. 3). From the intensity ratio of the 276-keV isomeric transi-

tion and the 356-keV transition following  $^{133}\text{Ba}^f$  decay, and the known half-lives of  $^{133}\text{Ba}^m$  and  $^{133}\text{Ba}^f$ , we estimate that 0.03% of all  $^{133}\text{La}$  decays lead to population of  $^{133}\text{Ba}^m$ ; an estimate lower than that of Harmatz and Handley. The uncertainty is approximately a factor of 2, and results primarily

TABLE II. Conversion coefficients deduced from the conversion electron intensities of Ref. 2 and experimentally determined  $\gamma$ -ray intensities.

Conversion line	$I_{ce}(\text{rel.})^a$	Conversion <sup>b</sup> coefficient	$\Lambda^c$	Conversion line	$I_{ce}(\text{rel.})^a$	Conversion <sup>b</sup> coefficient	$\Lambda^c$
113K	38	0.8	$E2, M1$	565K	35	0.0063	$E2(+M1)$
136K	7	0.4	$M1, E2$	567K	$\approx 8$	0.0045	(E2)
158K	4	0.28	$E2, M1$	584K	9	0.0054	$E2(+M1)$
210K	10	0.19		595K	30	0.0077	$M1(+E2)$
256K	16.5	0.9		618K	53	0.0061	$M1(+E2)$
278K	1000	0.0487	d	L	8	0.0009	
L <sub>1</sub>	145	0.0071		621K	22	0.0042	$E2(+M1)$
M	35	0.0017		L	3	0.0006	
286K	11	0.044	$M1, E2$	632K	58	0.0061	$M1(+E2)$
290K	520	0.045	$M1, E2$	L	<11	<0.0012	
L <sub>1</sub>	70	0.0060		751K	2.5	0.0054	$M1(+E2)$
M	18	0.0016		810K	0.9	0.002	$E2(+M1)$
291K	$\approx 120$	0.034	$E2(+M1)$	846K	11.6	0.0023	$E2(+M1)$
L <sub>1</sub>	$\approx 25$	0.006		850K	1.0	0.0034	$M1, E2$
302K	515	0.038	$M1(+E2)$	858K	11.0	0.0027	$M1, E2$
L <sub>1</sub>	80	0.0056		L	1.4	0.00034	
M	23	0.0017		911K	2.1	0.0015	$E2(+M1)$
353K	7	0.045		1009K	1.6	0.0021	$M1, E2$
385K	16.5	0.030	$M1(+E2)$	1061K	1.7	0.0020	$M1(+E2)$
L <sub>1</sub>	3	0.0054		1099K	3.4	0.0017	$M1, E2$
435K	5.5	0.026		1199K	0.8	0.0032	$M1, E2$
527K	5	0.0070	$E2(+M1)$	1211K	0.9	0.0020	$M1, E2$
534K	4	0.009	$M1, E2$	1284K	e		E1
556K	5	0.0047					

<sup>a</sup> Uncertainties were  $\pm 15\%$  for the strongest lines; see Ref. 2.

<sup>b</sup> Normalized to  $\alpha_K(278\gamma) = 0.0487$ ; if the 278 $\gamma$  is pure M1 or E2, this value is incorrect by 5%. The contribution to the total uncertainty in the deduced conversion coefficient is insignificant.

<sup>c</sup> Deduced from comparison of experimental and theoretical conversion coefficients.

<sup>d</sup> Multipolarity assumed to be 50% M1 + 50% E2.

<sup>e</sup> The K conversion electron intensity for an E1 transition is 0.3, for an E2 transition it is 0.67, and for an M1 transition it is 0.9.

TABLE III.  $\gamma$ -ray coincidences resulting from  $^{133}\text{La}$  decay.

Gate <sup>a</sup>	Coincident $\gamma$ rays
278	286, 339, 385, 567, 571, 595, 632, 920, 1061
290 + 291 <sup>b</sup>	560, 584, 595, 621, 632, 1061
302	556, (560) <sup>c</sup> , 584, 621, 810
339	278
527	481, 671
534	565
565 + 567	278, 290 + 291, 534, 751
584	290 + 291, 302
592	469
595	278, 290 + 291
618	721
621	290 + 291, 302
630 + 632	278, 290 + 291
664	435
751	565
810	290 + 291, 302
1061	278

<sup>a</sup> Gates were 3 to 6 keV wide, centered on the  $\gamma$  ray indicated.

<sup>b</sup> The energy resolution of the coincidence system could not distinguish between closely spaced doublets. It is usually clear from the decay scheme which member contributes to the observed coincidence.

<sup>c</sup> Coincident  $\gamma$  ray in parentheses appeared very weakly or was otherwise partially obscured.

from the low intensity of the 276-keV transition.

The  $^{133}\text{La}$  decay scheme is normalized with the assumption that total decay is the sum of the total  $\gamma$ -ray transition intensity to the ground state (excluding the 12.33-keV transition), the total  $\gamma$ -ray transition intensity to the 12.33-keV level, and the  $\epsilon + \beta^+$  decay intensity to the 12.33-keV level. Decay to the ground state is assumed to be negligible on the basis of the  $\Delta J = 2$ ,  $\Delta\pi = \text{no } \beta$  transition necessary to directly populate the  $^{133}\text{La}$  ground state. The  $\beta^+$  decay intensity is obtained from the annihilation peak intensity corrected for small contributions from  $\beta^+$  decay to the 291- and 302-keV levels. The  $\epsilon/\beta^+$  ratio is then obtained using the calculations of Gove and Martin.<sup>12</sup> The  $Q$  value necessary for the above determinations is 1900 keV and was obtained by Wapstra and Gove with systematics.<sup>13</sup> Total conversion coefficients were estimated from Hager and Seltzer.<sup>10</sup> The resulting normalization factor that gives intensities per 100 decays is  $N = 1.89 \times 10^{-3} \pm 8 \times 10^{-5}$ . A change of 100 keV in the assumed  $Q$  value results in an additional uncertainty of  $6.7 \times 10^{-4}$ .

The  $\log ft$  values were determined from the intensity balance at each excited level. The  $Q$  value is again 1900 keV and the  $^{133}\text{La}$  half-life is 3.912 h. An uncertainty of 100 keV in the  $Q$  value introduces an uncertainty of less than 0.1 in the  $\log ft$  value

for levels below 1500 keV, though the absolute decay branches are uncertain by more than 30%. The decay branches and  $\log ft$  values are summarized in Fig. 2.

The spins and parities of the  $^{133}\text{Ba}$  ground state, the 12.33-keV level, and the 288.38-keV level are  $\frac{1}{2}^+$ ,  $\frac{3}{2}^+$ , and  $\frac{11}{2}^-$ , respectively.<sup>1</sup> The  $^{133}\text{La}$  ground state has a spin of  $\frac{7}{2}$ ,<sup>2</sup> and the parity is positive, as required by the allowed  $\beta$  decay to the 12.33-keV level. Spins, parities, or their limits are deduced for many levels in  $^{133}\text{Ba}$  from the  $\log ft$  values,<sup>14</sup> by transition multipolarities determined from internal conversion coefficients, by systematics, and by the  $\gamma$ -ray decay characteristics. These assignments are summarized below.

**291.18-keV level.** The  $\log ft$  value and the observation of a ground state transition restrict  $J^\pi$  to  $\frac{5}{2}^+$  or  $\frac{3}{2}^+$ . Negative parity is not expected for low spin levels at the same energy as the  $h_{11/2}$  single-particle level. On the basis of systematics, the  $\frac{5}{2}^+$  assignment is preferred because the 302.38-keV level has  $J^\pi = \frac{3}{2}^+$ . The  $K$ -conversion coefficient of the 291.17-keV transition, though quite uncertain, is consistent with an  $E2$  transition.

**302.36-keV level.** The  $\log ft$  value and the  $M1(+E2)$  multipolarity of the 302.38-keV transition restrict  $J^\pi$  to  $\frac{3}{2}^+$ .

**539.88-keV level.** Zero  $\beta$  feeding suggests that  $J = \frac{1}{2}$ . The multipolarity of the 527.51-keV transition is  $E2(+M1)$  from the  $K$  internal conversion coefficient so the parity is positive. This level probably corresponds to the  $\frac{1}{2}^+$  level at 500 keV observed in  $(d, p)$  studies.<sup>5</sup>

**577.56-keV level.** The  $\log ft$  value of 7.4 limits  $J$  to  $\frac{3}{2}$ ,  $\frac{5}{2}$ , or  $\frac{7}{2}$ . The  $M1, E2$  transition to the  $\frac{5}{2}^+$  291.15-keV level, the  $E2$  transition to the  $\frac{3}{2}^+$  12.31-keV level, and the lack of a ground state transition indicate that this level is  $\frac{7}{2}^+$ .

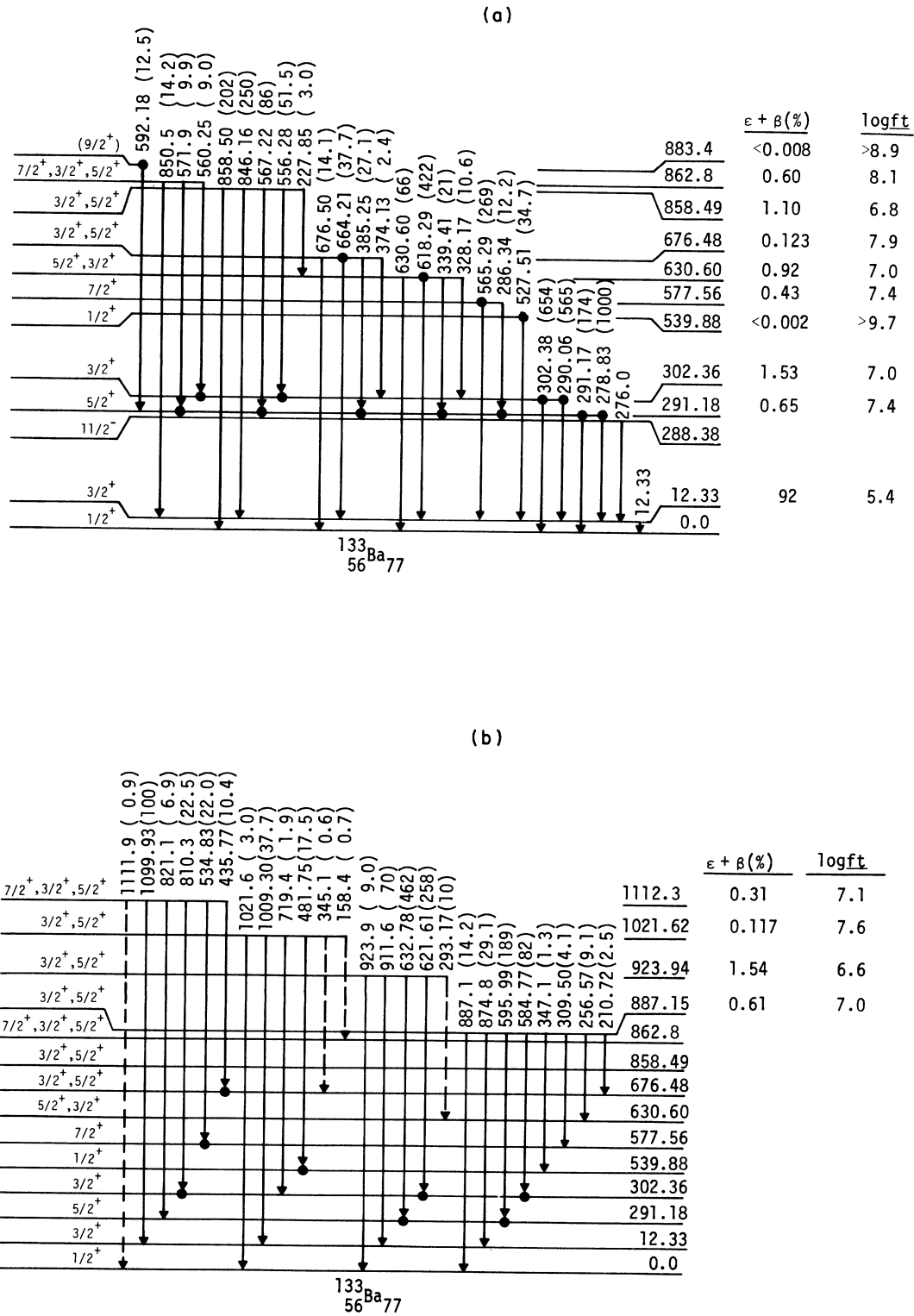
**630.60-keV level.** The  $\log ft$  value and the ground state transition restrict the spin to  $\frac{3}{2}$  or  $\frac{5}{2}$ . The  $M1(+E2)$  multipolarity of the 618.28-keV transition requires positive parity. We prefer a  $J^\pi$  assignment of  $\frac{5}{2}^+$  because of the identical  $\gamma$ -ray values branching to the known  $\frac{5}{2}^+$  level at 722.89 keV in  $^{131}\text{Xe}$  (Ref. 15); however,  $\frac{3}{2}^+$  cannot be entirely excluded.

**676.48-keV level.** The  $\log ft$  value and the  $M1(+E2)$  385.29-keV transition restrict  $J$  to  $\frac{3}{2}^+$  or  $\frac{5}{2}^+$ .

**858.49-keV level.**  $\log ft$  value and conversion coefficients of the 858.50- and 846.16-keV levels limit  $J^\pi$  to  $\frac{3}{2}^+$  or  $\frac{5}{2}^+$ .

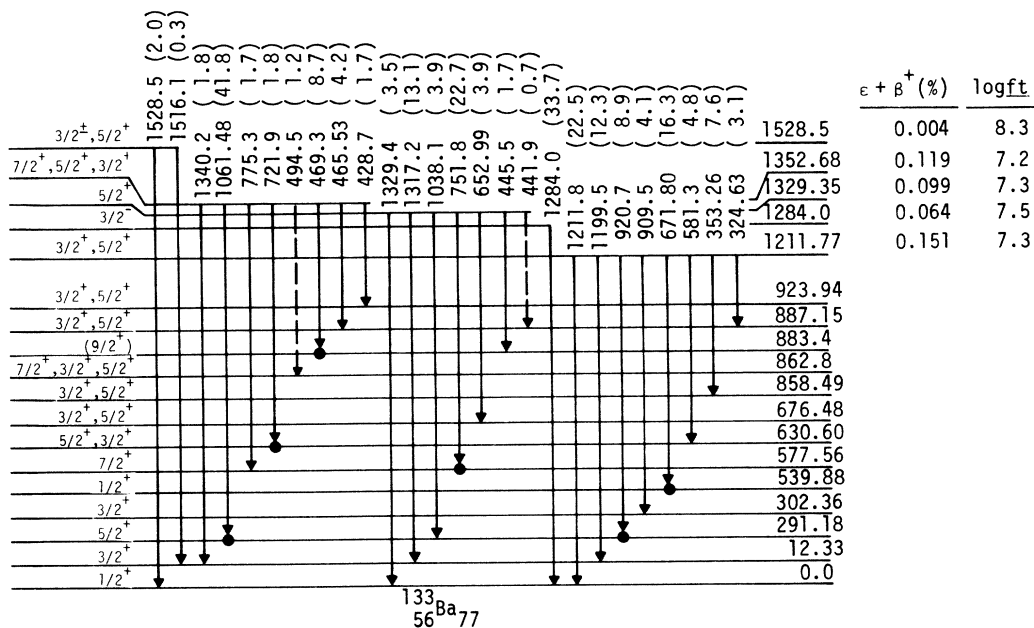
**862.8-keV level.** The  $\log ft$  value and the  $M1, E2$  850.5-keV transition indicate  $J^\pi = \frac{3}{2}^+$ ,  $\frac{5}{2}^+$ , or  $\frac{7}{2}^+$ . The lack of a ground state transition favors  $\frac{7}{2}^+$ .

**883.4-keV level.** The decay to only the  $\frac{5}{2}^+$  291.18-keV level suggests that this level has  $J$



FIGS. 2. (a)-(d) The  $^{133}\text{Ba}$  level scheme showing  $\epsilon + \beta^+$  decay branches,  $\log ft$  values, and relative photon intensities.

(c)



(d)

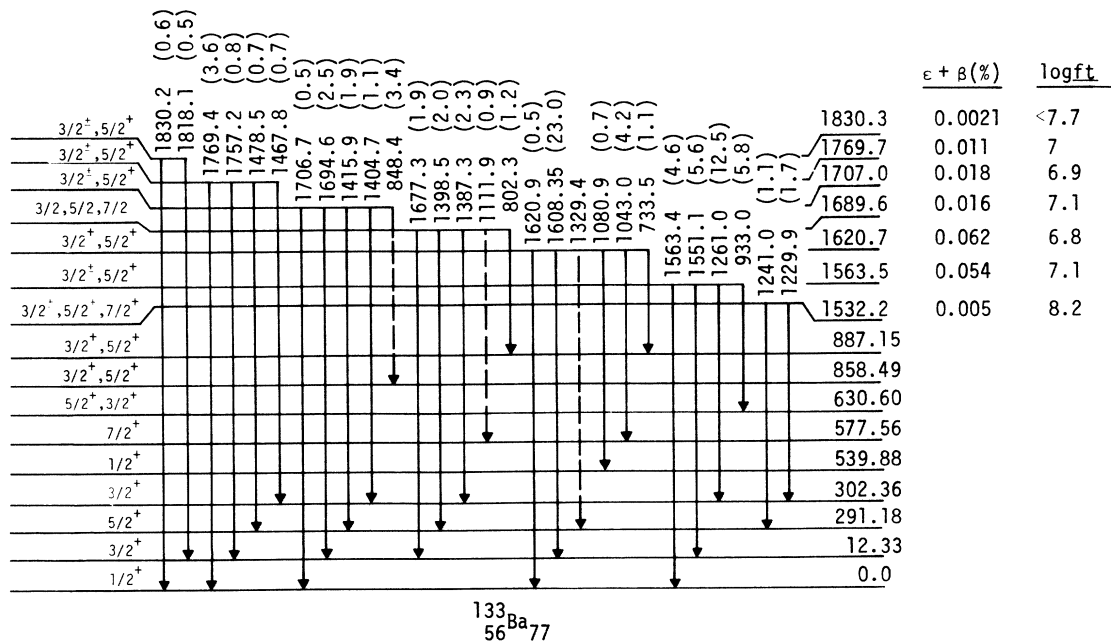


FIG. 2 (Continued)

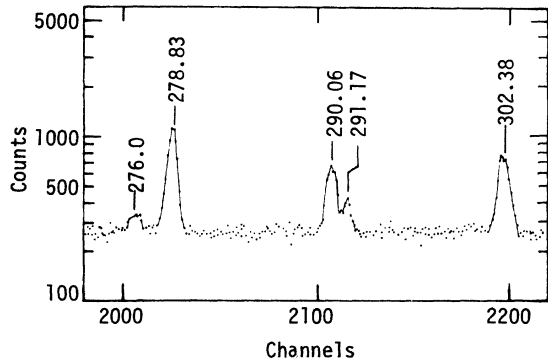


FIG. 3. A portion of the low-energy  $\gamma$ -ray spectrum taken with the LEPS. This spectrum, taken after approximately six half-lives of  $^{133}\text{La}$ , shows the 276-keV  $^{133}\text{Ba}$  isomeric transition and the intense photopeaks from  $^{133}\text{La}$  decay in this region.

$=\frac{9}{2}^+$ . Possible transitions to the  $\frac{7}{2}^+$  or  $\frac{11}{2}^-$  levels would be obscured by other intense transitions. Upper limits of 0.3 and 0.9 relative units can be placed on transitions to the ground state and 12.33-keV level, respectively.

**887.15-keV level.** The  $\log ft$  value, the observed ground state transition, and the  $M1(+E2)$  595.99-keV transition restrict  $J^\pi$  to  $\frac{3}{2}^+$  or  $\frac{5}{2}^+$ .

**923.94-keV level.** The  $\log ft$  value, the observed ground state transition, and the  $M1(+E2)$  632.78-keV transition give  $J^\pi = \frac{3}{2}^+$  or  $\frac{5}{2}^+$ .

**1021.62-keV level.** The  $\log ft$  value and the  $M1$  or  $E2$  1009.30-keV transition limit  $J^\pi$  to  $\frac{3}{2}^+$  or  $\frac{5}{2}^+$ .

**1112.3- and 1352.68-keV levels.**  $\log ft$  values limit  $J$  to  $\frac{3}{2}$ ,  $\frac{5}{2}$ , or  $\frac{7}{2}$ . The  $M1$  or  $E2$  transitions to positive parity levels indicate a positive parity for both levels. Lack of definite ground state transitions suggests the  $\frac{7}{2}$  spin is possible. If the 883.4-keV level is  $\frac{9}{2}^+$ , the 1352.68-keV level cannot be  $\frac{3}{2}^+$ .

**1211.77-keV level.** The  $\log ft$  value and  $M1$  or  $E2$  transitions to both the ground state and the 12.33-keV levels restrict  $J^\pi$  to  $\frac{3}{2}^+$  or  $\frac{5}{2}^+$ .

**1284.0-keV level.** The  $\log ft$  value and the ground state transition limit  $J^\pi$  to  $\frac{3}{2}^+$  or  $\frac{5}{2}^+$ . Harmatz and Handley do not report a  $K$ -conversion line for this transition, though they do report one for the 1199.45-keV transition, which has a photon intensity one-third that of the 1284.0-keV transition. This indicates that the 1284.0-keV transition is  $E1$  and limits  $J^\pi$  to  $\frac{3}{2}^-$ .

**1329.35-keV level.** The  $\log ft$  value,  $M1(+E2)$  751.8-keV transition, and the ground state transition restrict  $J^\pi$  to  $\frac{5}{2}^+$ .

**1528.5-, 1563.5-, 1707.0-, 1769.7-, and 1830.3-keV levels.** The  $\log ft$  values and the observation of the ground state transitions restrict  $J^\pi$  to  $\frac{3}{2}^+$  or  $\frac{5}{2}^+$  for these levels.

**1532.2-keV level.** The  $\log ft$  value and the ob-

served transitions limit  $J^\pi$  to  $\frac{7}{2}^+$ ,  $\frac{5}{2}^+$ , or  $\frac{3}{2}^+$ .

**1620.7-keV level.** The  $\log ft$  value and the transitions to both the  $\frac{1}{2}^+$  ground state and  $\frac{7}{2}^+$  577.56-keV level limit  $J^\pi$  to  $\frac{3}{2}^+$  or  $\frac{5}{2}^+$ .

**1689.6-keV level.** The  $\log ft$  value limits  $J$  to  $\frac{3}{2}$ ,  $\frac{5}{2}$ , or  $\frac{7}{2}$ .

In addition to the above levels, we specifically looked for a level at  $794 \pm 10$  keV observed in  $(d, p)$  reactions by von Ehrenstein *et al.*<sup>5</sup> They reported an  $l$  transfer of 3, indicating  $J^\pi = \frac{5}{2}^-$  or  $\frac{7}{2}^-$ . Such a level could be populated from a  $\frac{5}{2}^+$  parent by either direct  $\beta$  decay or through  $\gamma$ -ray cascades. If the level reported at 794 keV has  $J^\pi = \frac{7}{2}^-$ , it could be largely responsible for populating the  $\frac{11}{2}^-$  isomeric level. The observed population of the  $\frac{11}{2}^-$  level is equivalent to  $16 \pm 8$  relative intensity units. The only  $\gamma$  ray not placed that could depopulate a level at this energy is the 519.1-keV  $\gamma$  ray with a relative intensity of  $9 \pm 3$ . The resulting 807.3-keV level might also populate the  $\frac{5}{2}^+$  291.15-keV level by a 516-keV transition. This  $\gamma$  ray, if present, is very weak and not resolvable from the annihilation peak. No other observed transitions could feed a level at 807.3 keV, including an expected  $E2$  transition from the  $\frac{3}{2}^-$  1284.0-keV level.

If the 794-keV level reported in  $(d, p)$  work has  $J^\pi = \frac{5}{2}^-$ , it could decay by  $E1$  transitions to the 12.31-, 291.15-, and 302.38-keV levels. A  $\gamma$  ray at 494.5 keV is tentatively placed as depopulating the 1352.6-keV level. If this transition feeds the 291.15- or 302.38-keV levels, a level at 785.7-, or 796.9 keV would result. In neither case are additional possible transitions populating or depopulating such levels found.

Thus, the existence of a  $\frac{5}{2}^-$  or  $\frac{7}{2}^-$  level at approximately 800 keV cannot be supported from these  $\beta$ -decay data.

#### IV. DISCUSSION

##### Comparison with previous studies

This work confirms the 12  $^{133}\text{Ba}$  levels deduced by both previous decay studies and 3 other levels reported only by Reuland and Pagliughi. We also report 13 new levels. No basis was found for establishing levels at 1139, 1296, 1607, and 1679 keV as reported by Reuland and Pagliughi, or at 435, 1101, 1642, 1647, and 1875 keV as reported by Harmatz and Handley. Many of the transitions on which these levels were based are placed elsewhere in the present level scheme.

Our  $\beta$ -decay study reports many of the same levels observed in the  $(d, p)$  reaction work of von Ehrenstein *et al.* However, the reported  $l$ -transfer values require  $J$  values not in agreement with those we propose for several levels. The good energy agreement for levels populated by these



two methods indicates that doublet levels are probably not involved.

From the  $(d, p)$  study, the 858.47-keV level and possibly the 887.14-keV level would have  $J^\pi = \frac{1}{2}^-$  or  $\frac{3}{2}^-$ . In each case  $J^\pi = \frac{1}{2}^-$  requires a pure  $M2$  transition out of the level and pure  $M2$  transitions cannot be accommodated by the internal conversion data. If the 858.47- and 887.14-keV levels are  $\frac{3}{2}^-$ , the 846.16-, 858.50-, 595.99-, and 584.77-keV transitions would have to have 19, 26, 32, and 16%  $M2$  admixtures, respectively, to reproduce the experimental  $K$ -conversion coefficients. This requirement for unusually large  $M2$  admixtures indicates that the  $l$ -transfer values reported for these levels are unlikely to be correct. Hopefully, further reaction studies will rectify these discrepancies.

#### Even parity levels of $^{133}\text{Ba}$

The low-lying positive parity levels in  $^{133}\text{Ba}$  can be qualitatively accounted for by considering the low-lying single-particle levels and the coupling of these single-particle levels to the  $^{132}\text{Ba}$  core.

The ground state and the first excited state can be identified with the  $3s_{1/2}$  and  $2d_{3/2}$  single-particle orbitals. The  $\frac{3}{2}^+$  level at 12.33 keV has a half-life of  $8.1 \pm 2.0$  ns and its deexcitation by a 12.33-keV  $M1$  transition is hindered by a factor of 50.

Such a hindrance is consistent with a  $2d_{3/2}$  to  $3s_{1/2}$  transition in this region.<sup>16</sup> The remaining positive parity levels below 700 keV can be accounted for by coupling these two single-particle levels to the first  $2^+$  core level at 464.69 keV in  $^{132}\text{Ba}$ .

Between 700 and 1360 keV there are nine levels with  $J^\pi = \frac{3}{2}^+$ ,  $\frac{5}{2}^+$ , or  $\frac{7}{2}^+$ , and one level with a possible  $J^\pi = \frac{9}{2}^+$ . All but two levels with  $\frac{3}{2}^+$  or  $\frac{5}{2}^+$  can result from coupling the  $3s_{1/2}$  and  $2d_{3/2}$  single-particle levels to the  $2_2^+$  and  $4_1^+$  core levels at 1031.77 and 1127.82 keV in  $^{132}\text{Ba}$ . To accommodate the two additional  $\frac{3}{2}^+$  or  $\frac{5}{2}^+$  levels, the  $2d_{5/2}$  or  $1g_{7/2}$  single-particle levels or higher-lying core states have to be included. Thus, qualitatively positive parity levels with the observed spin and parity values can be explained by a weak-coupling model. There is substantial mixing between such states, however, because several of the "second phonon" levels have transitions to single-particle levels. In addition, several levels from the suggested couplings are 200 keV or more from the particle-plus-core state energy.

#### Odd parity levels of $^{133}\text{Ba}$

Because the low-lying  $^{133}\text{La}$  negative parity states are described by a particle-plus-asymmetric-rotor model,<sup>17-19</sup> this model might describe the

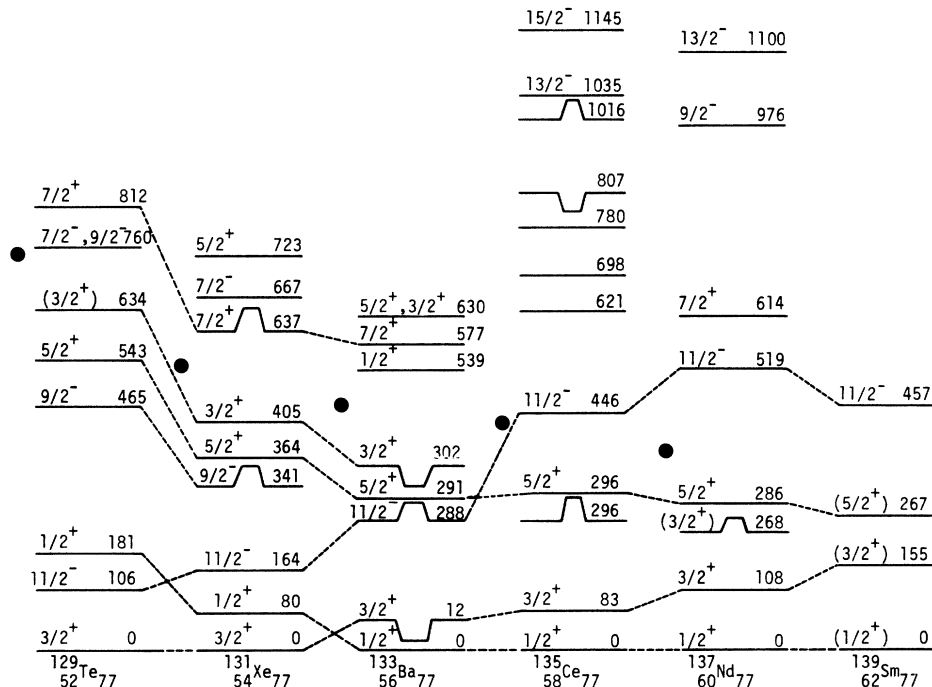


FIG. 4. Systematics of the  $N=77$  nuclei from  $Z=52$  to  $Z=62$ . The dot to the left of each level diagram indicates the energy of the  $2_1^+$  state in the even-even core nucleus.

$^{133}\text{Ba}$  negative parity states as well. It is known that  $^{130}\text{Ba}$  and  $^{134}\text{Ba}$  have prolate deformation.<sup>20</sup> In  $^{133}\text{La}$  an odd proton is coupled to the  $^{132}\text{Ba}$  core and the  $h_{11/2}$  proton state is observed. In  $^{133}\text{Ba}$  an odd neutron is coupled to the  $^{132}\text{Ba}$  core and the  $h_{11/2}$  neutron state is observed. One might expect negative parity level structures similar to those in  $^{133}\text{La}$  to appear in  $^{133}\text{Ba}$ .

The only negative parity level we observed in  $^{133}\text{Ba}$ , in addition to the  $h_{11/2}$  single neutron level, was the  $\frac{3}{2}^-$  1284.0-keV level, which is 996 keV above the  $\frac{1}{2}^-$  single-particle level. The  $4_1^+$  core state is at 1128 keV. Thus, if we assume that the 1284.0-keV level is the  $\frac{3}{2}^-$  level associated with the  $h_{11/2}$  single particle coupled to a deformed core, the core is either symmetric prolate or triaxial. For an oblate shape, the  $\frac{3}{2}^-$  level rises rapidly above the  $h_{11/2} + 4_1^+$  oblate core energy as  $\beta$  decreases and the core is deformed from the symmetric shape.<sup>18</sup>

#### Systematics of the $N=77$ nuclei

The systematics of the low-lying levels of the  $N=77$  nuclei<sup>15,21-23</sup> are shown in Fig. 4. The energies of the  $2_1^+$  even-even core states are indicated by heavy dots. A number of the even parity levels follow the general compression of level density as the proton number is increased from  $^{129}\text{Te}$  to  $^{133}\text{Ba}$ . However, after  $^{133}\text{Ba}$ , gross features remain the same through  $^{139}\text{Sm}$ , except for the slow separation of the first  $\frac{1}{2}^+$  and  $\frac{3}{2}^+$  levels. The first  $\frac{5}{2}^+$  level remains remarkably constant in energy from  $^{133}\text{Ba}$  to  $^{139}\text{Ce}$ . Because the even-even core  $2_1^+$  level is also constant, this suggests the first  $\frac{5}{2}^+$  state has as its primary configuration the  $3s_{1/2}$  single-particle state coupled to the  $2_1^+$  core state. It also

suggests that the second  $\frac{5}{2}^+$  level at 722 keV in  $^{131}\text{Xe}$  and the possible  $\frac{5}{2}^+$  level at 630 keV in  $^{133}\text{Ba}$  arise mostly from the  $2d_{3/2}$  single-particle state coupled to the  $2_1^+$  core state, although the modest branching from the  $\frac{5}{2}^+$  level to the  $\frac{3}{2}^+$  level does indicate some mixing. We discuss these properties elsewhere.<sup>24</sup>

In contrast to the smooth variation of the even parity levels, the odd parity levels undergo a dramatic change from  $^{129}\text{Te}$  to  $^{137}\text{Nd}$ . The  $h_{11/2}$  single-particle state is seen in all the nuclei shown in Fig. 4; however, the levels built on this state are quite different. In  $^{129}\text{Te}$  and  $^{131}\text{Xe}$  the low-lying  $\frac{9}{2}^-$  and  $\frac{7}{2}^-$  levels can be accounted for by weak coupling models such as that of Kisslinger and Sorenson<sup>25</sup> or the multiparticle model of Kuriyama, Marumori, and Matsuyanagi.<sup>26</sup> On the basis of these systematics, a  $\frac{7}{2}^-$  level at 807 keV in  $^{133}\text{Ba}$  might be reasonable.

Recent calculations with the particle-plus-asymmetric-rotor model have reproduced the heavily distorted odd parity yrast band with  $h_{11/2}$  parentage in  $^{137}\text{Nd}$ . Other odd parity levels appearing in  $^{137}\text{Nd}$  might be attributed to states with  $h_{9/2}$  parentage within an asymmetric nucleus. In-beam reaction studies of  $^{135}\text{Ce}$  levels suggest a similar nature for the odd parity levels in that nucleus.

The  $^{133}\text{Ba}$  nucleus resides in between these two regions. As we have shown, the even parity level properties of  $^{133}\text{Ba}$  are consistent with those of the heavier nuclei. It is clear that further studies, such as in-beam  $\gamma$ -ray spectroscopy studies, are necessary to explore the negative parity levels in  $^{133}\text{Ba}$  and to find if the negative parity level structures of  $^{133}\text{Ba}$ ,  $^{133}\text{La}$ , and the heavier  $N=77$  nuclei are indeed similar.

\*This work was performed under the auspices of the U. S. Energy Research and Development Administration, under Contract No. W-7405-Eng-48.

<sup>1</sup>G. P. Nowicki, Ges. F. Kernforschung Karlsruhe, West Germany, Report No. KFK-2017, (1974) (unpublished).

<sup>2</sup>E. A. Henry, Nucl. Data Sheets **11**, 495 (1974).

<sup>3</sup>B. Harnatz and T. H. Handley, Nucl. Phys. **81**, 481 (1966).

<sup>4</sup>D. J. Reuland and D. W. Pagliughi, J. Inorg. Nucl. Chem. **35**, 1777 (1973).

<sup>5</sup>D. von Ehrenstein, G. C. Morrison, J. A. Noland, Jr., and N. Williams, Phys. Rev. C **1**, 2066 (1970).

<sup>6</sup>E. A. Henry, N. Smith, P. G. Johnson, and R. A. Meyer, Phys. Rev. C **12**, 1314 (1975).

<sup>7</sup>R. Gunnick and J. B. Niday, Lawrence Livermore Laboratory Report No. UCRL-51061, I-IV, 1971, 1972 (unpublished).

<sup>8</sup>W. A. Myers and R. J. Nagle, J. Inorg. Nucl. Chem. **35**, 3985 (1973).

<sup>9</sup>J. B. Niday and L. G. Mann, in *Radioactivity in Nuclear*

*Spectroscopy*, edited by J. H. Hamilton and J. C. Manthuruthil (Gordon and Breach, New York, 1972), Vol. **1**, p. 313.

<sup>10</sup>R. S. Hager and E. C. Seltzer, Nucl. Data **A4**, 1 (1968).

<sup>11</sup>R. J. Nagle (private communication).

<sup>12</sup>N. B. Gove and M. J. Martin, Nucl. Data **A10**, 206 (1971).

<sup>13</sup>A. H. Wapstra and N. B. Gove, Nucl. Data **A9**, 267 (1971).

<sup>14</sup>S. Raman and N. B. Gove, Phys. Rev. C **1**, 1995 (1973).

<sup>15</sup>R. A. Meyer, F. Momyer, and W. B. Walters, Z. Phys. **268**, 387 (1974).

<sup>16</sup>J. S. Geiger, R. L. Graham, I. Bergström, and F. Brown, Nucl. Phys. **68**, 352 (1965).

<sup>17</sup>E. A. Henry and R. A. Meyer, Z. Phys. **271**, 75 (1974).

<sup>18</sup>J. Meyer-ter-Vehn, Nucl. Phys. **A249**, 111, 141 (1975).

<sup>19</sup>J. R. Leigh, K. Nakai, K. H. Maier, F. Puhlhofer, F. S. Stephens, and R. M. Diamond, Nucl. Phys. **A213**, 1 (1973).

<sup>20</sup>M. Nieman, R. Kalish, D. R. S. Somayajulu, B. Hers-

- kind, F. Genovese, and L. Grodzins, *Phys. Lett.* 52B, 189 (1974).
- <sup>21</sup>D. J. Horen, ORNL Report No. ORNL-4730, 1971 (unpublished).
- <sup>22</sup>R. Arlt, G. Beyer, V. A. Morozov, H. Musiol, T. M. Muminov, H. Tyrroff, H. Strusny, Z. A. Usmanova, V. I. Fominykh, H. Fuya, A. B. Khalikulov, and E. Herrmann, *Izv. Akad. Nauk. SSSR Ser. Fiz.* 36, 744 (1972) [*Bull. Acad. Sci. USSR Phys. Ser.* 36, 673 (1973)].
- <sup>23</sup>J. Gizon, A. Gizon, M. R. Maier, R. M. Diamond, and F. S. Stephens, *Nucl. Phys.* A222, 557 (1974).
- <sup>24</sup>R. A. Meyer, J. H. Landrum, E. A. Henry, R. P. Yaffe, and W. B. Walters, Lawrence Livermore Laboratory Preprint UCRL-76898 (unpublished).
- <sup>25</sup>L. S. Kisslinger and R. A. Sorenson, *Rev. Mod. Phys.* 35, 853 (1963).
- <sup>26</sup>A. Kuriyama, T. Marumori, and K. Matsuyanagi, Institute for Nuclear Study, University of Tokyo Report No. INS-204, 1973 (unpublished).